

# Balmer lines as $T_{\text{eff}}$ and $\log g$ indicators for non-solar composition atmospheres

## An application to the extremely helium-weak star HR 6000<sup>\*</sup>

G. Catanzaro<sup>1</sup>, F. Leone<sup>1</sup>, and T. H. Dall<sup>2</sup>

<sup>1</sup> INAF - Catania Astrophysical Observatory, via S. Sofia 78, 95123 Catania, Italy  
e-mail: [gcatanzaro; fleone]@ct.astro.it

<sup>2</sup> European Southern Observatory, Casilla 19001, Santiago 19, Chile  
e-mail: tdall@eso.org

Received 30 March 2004 / Accepted 11 June 2004

**Abstract.** Although the importance of a correct abundance assumption in the determination of effective temperature and surface gravity of a star has been demonstrated in the literature, this determination is often still extremely simplified, neglecting the effects of non-solar chemical abundances. In this paper we show how the modeling of the profiles of  $H_\delta$  and  $H_\gamma$ , commonly used as  $T_{\text{eff}}$  and  $\log g$  indicators, is affected when the chemical composition is far from the standard one. As a target for our study we selected the chemically peculiar star HR 6000. Comparing the observed and synthetic profiles of  $H_\delta$  and  $H_\gamma$  we obtained  $T_{\text{eff}} = 12\,950$  K and  $\log g = 4.05$ ; the atmospheric model has been computed with a metal opacity scale evaluated for  $[M/H] = -0.5$  and  $\text{He}/\text{H} = 0$ . A number of FeII lines have been used to infer the rotational velocity ( $v_e \sin i = 0 \text{ km s}^{-1}$ ) and the heliocentric radial velocity ( $RV = 0.67 \text{ km s}^{-1}$ ). By requiring that the abundance of iron is independent of the 96 measured equivalent widths, we determined the microturbulence velocity ( $\xi = 0 \text{ km s}^{-1}$ ). The abundance pattern coming from our study is similar to the one inferred from UV lines by Castelli et al. (1985), with the exception of O, Al, Si, Sc and Ni. Possible causes for these discrepancies are discussed. With respect to the Sun, we found the iron peak elements to be normal or overabundant and the light elements, with the exception of Na and P, to be extremely underabundant. We find that HR 6000 is one of the most He-underabundant among the chemically peculiar stars.

**Key words.** stars: fundamental parameters – stars: individual: HR 6000 – stars: chemically peculiar – stars: atmospheres – stars: abundances

## 1. Introduction

Unevolved early-type stars play a key role in many aspects of modern astrophysics. Since their radiative atmospheres are particularly stable, their surface abundances reflect those of the formation regions from which they originated. Hence, a correct determination of these abundances is the primary task to fulfil in any study – from the chemical gradient in the Milky-Way to the evolution of external galaxies.

To perform a detailed and quantitative abundance analysis of a stellar atmosphere, a precise determination of the effective temperature and surface gravity is mandatory. Erspamer & North (2003) found that even a 150 K error in the effective temperature results in a 0.1 dex error in the derived abundances. A similar abundance error is made when the gravity is wrong by 0.2 dex only.

One of the most accurate methods commonly used to infer  $T_{\text{eff}}$  and  $\log g$  is based on the comparison of the observed and theoretical profiles of Balmer lines. Several studies have shown that a non-standard chemical composition of the stellar atmosphere alters the flux distribution of the star (Leckrone et al. 1974) or modifies the profiles of the Balmer lines (Leone & Manfré 1997). The latter authors found that the  $H_\beta$  line profile depends on the metal and helium abundances. Hence, the metal opacity scale and the microturbulence velocity adopted to compute the atmosphere model have to be consistent with the derived abundances, measured microturbulence,  $T_{\text{eff}}$  and  $\log g$ .

Here we extend the method of Leone & Manfré (1997), adding the advantage of matching the two important Balmer lines,  $H_\delta$  and  $H_\gamma$ , in the determination of  $T_{\text{eff}}$  and  $\log g$ . We investigate how an extremely non standard atmosphere can influence the determination of the fundamental parameters. With this aim we extracted HR 6000 from a sample of high resolution spectroscopic observations collected by us within our program dedicated to chemically peculiar (CP) stars. This

<sup>\*</sup> Based on observations collected at European Southern Observatory (ESO), La Silla, Chile, proposal ID 69.D-0537.

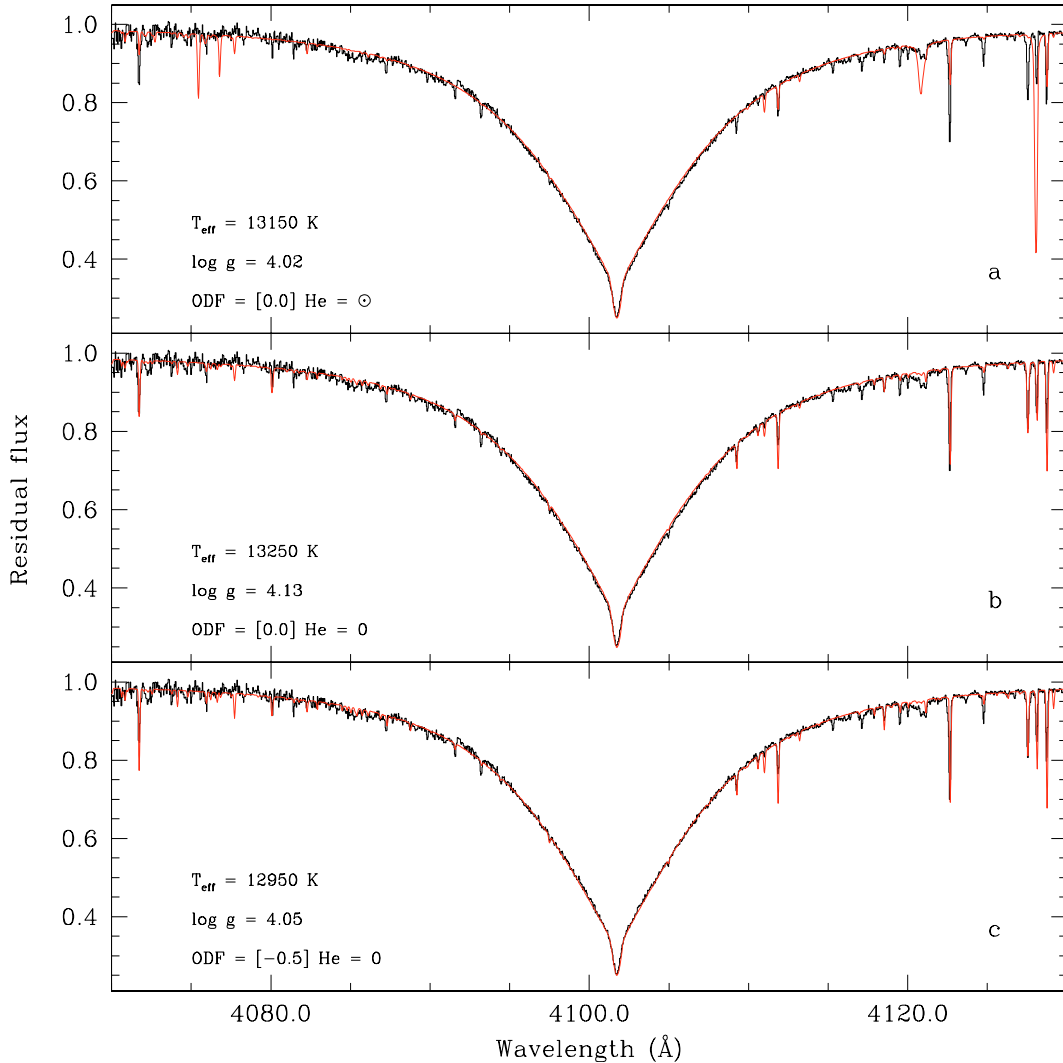


**Fig. 1.** Comparison between the observed and computed  $H_{\delta}$  line profile. Each profile has been calculated using models with different ODF tables.

object has been selected for its complicated abundance pattern (Andersen et al. 1984; Castelli et al. 1985) that makes its atmosphere completely different from the solar case. The star will be described in the next section.

## 2. HR 6000 = HD 144667

According to the first classification by Bessel & Eggen (1972), HR 6000 is a chemically peculiar star belonging to the He-weak subgroup. From the spectroscopic point of view, two studies have been published: a qualitative analysis of its optical spectrum by Andersen et al. (1984) and the IUE-based analysis by Castelli et al. (1985), who were the first to provide an accurate quantitative abundance pattern of the object. From these analyses it is clear that HR 6000 does not fit any of the classes of CP stars as defined by Preston (1974), although it shares some characteristics typical of both the HgMn and the He-weak phosphorous stars.

HR 6000 and HR 5999 form the common proper motion visual double system *Dunlop 199* located in the Lupus 3 association. The latter object has been studied by Thè & Tjin A Djie (1978) and Tjin A Djie & Thè (1978), who found that it is

probably a pre-main sequence star in the contracting stage with an age of about  $7 \times 10^5$  years. If these two stars are coeval, HR 6000 is one of the youngest objects among the known CP stars. This result allows us to set a lower limit for the age when the chemical peculiarities arise in the atmosphere of this class of objects.

van den Ancker et al. (1996) suggested the presence of a cool (K or M type) companion close to HR 6000 to explain the infrared excess and the X-ray emission discovered by the EXOSAT (Thè et al. 1985) and ROSAT (Zinnecker & Preibisch 1994) satellites. Moreover, according to the formation region where HR 6000 is located, they concluded that its invisible companion should be a T Tauri star about 6 mag fainter than the primary and will thus not contribute significantly to the total luminosity of the system.

## 3. Observations and data reduction

A spectrum of HR 6000 in the 3600–9200 Å spectral range was obtained with the FEROS spectrograph on August 29, 2002 at the ESO 1.52 m telescope at La Silla Observatory, Chile. The spectral resolution was  $R = 48\,000$ .

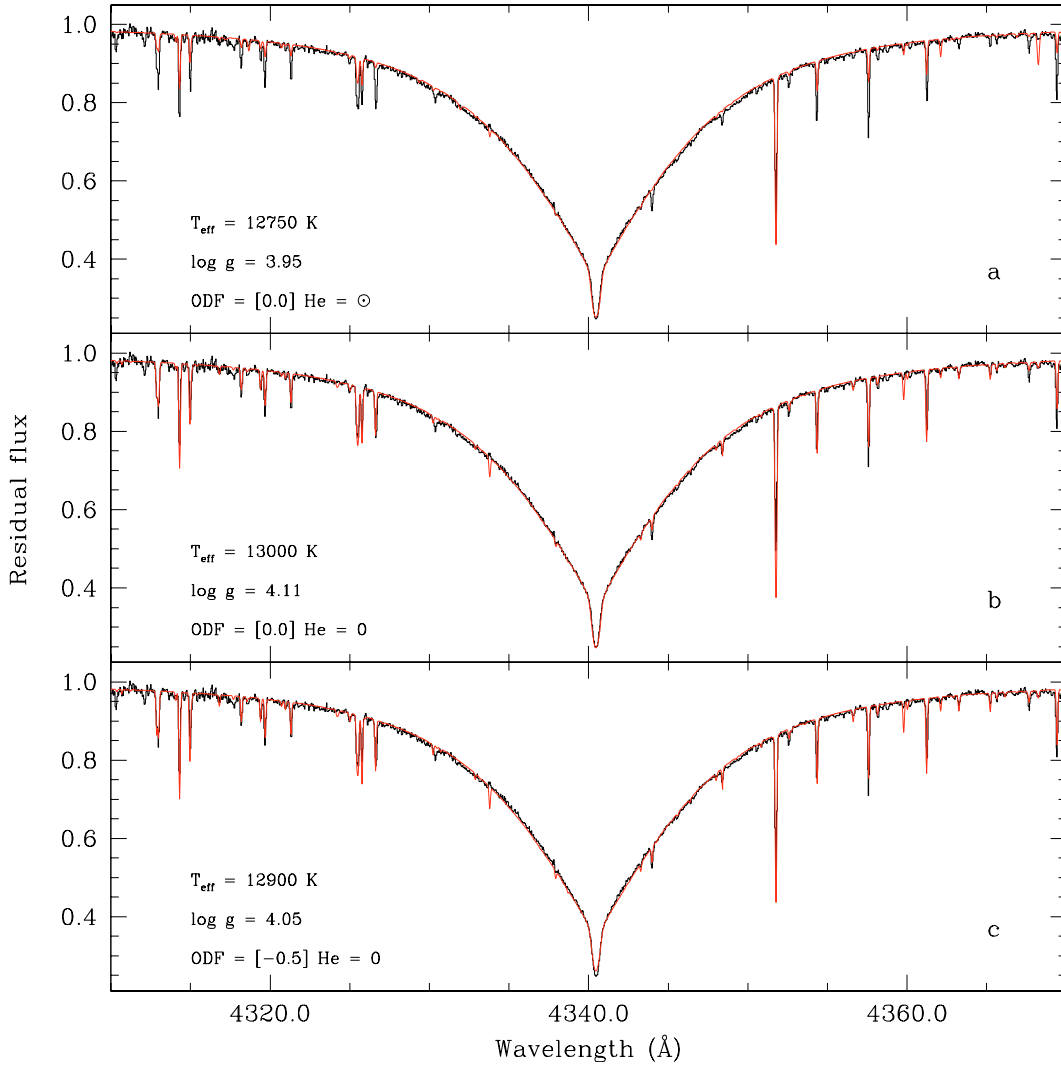


**Fig. 2.** As in the Fig. 1 but for  $H_\gamma$  line profile.

The stellar spectrum, wavelength calibrated and normalized to the continuum, was obtained using standard data reduction procedures for spectroscopic observations within the NOAO/IRAF package. For our analysis we considered the interval 3800–7000 Å which is free of fringing and where  $S/N \geq 100$ .

#### 4. Atmospheric parameters

The approach we used in this paper was to minimize the difference between observed and synthetic  $H_\delta$  and  $H_\gamma$  profiles. As goodness-of-fit test we used the parameter:

$$\chi^2 = \frac{1}{N} \sum \left( \frac{I_{\text{obs}} - I_{\text{th}}}{\delta I_{\text{obs}}} \right)^2$$

where  $N$  is the total number of points,  $I_{\text{obs}}$  and  $I_{\text{th}}$  are the intensities of the observed and computed profiles, respectively, and  $\delta I_{\text{obs}}$  is the photon noise. The synthetic spectra were generated in three steps: first, we computed the stellar atmosphere model by using the ATLAS9 code (Kurucz 1993) then, the stellar spectrum was synthesized using SYNTHE

(Kurucz & Avrett 1981) and finally, the instrumental and rotational convolutions were applied. The ATLAS9 code includes the metal opacity by means of distribution functions (ODF) that are tabulated for multiples of the solar metallicity and for various microturbulence velocities in the Kurucz web site<sup>1</sup>.

Leone & Manfré (1997) determined  $T_{\text{eff}}$ ,  $\log g$ , microturbulence velocity and abundances, minimizing  $\chi^2$  adopting an iterative procedure, but for  $H_\beta$  alone.

Unfortunately in FEROS spectra the  $H_\beta$  line of a B-type star is incomplete, in this study we extend this method to  $H_\delta$  and  $H_\gamma$ . The intersection of the two  $\chi^2$  iso-surfaces is expected to improve the final solution. Thus, to determine stellar parameters as consistent as possible with the actual structure of the atmosphere, we have reproduced the Balmer lines by the following iterative procedure:

- a) determination of  $T_{\text{eff}}$  and  $\log g$  of the ATLAS9 atmosphere model whose  $H_\delta$  and  $H_\gamma$  profiles, computed with SYNTHE, match the observations (see also panels a of Figs. 1 and 2). The model has been computed using the opacity scale and abundances of the Sun;

<sup>1</sup> <http://kurucz.harvard.edu/opacities.html>

- b) helium and metal abundances are derived and the microturbulent velocity determined from 96 FeII lines by requiring that the derived iron abundance does not depend on the measured equivalent widths;
- c) from the previous step we found an extreme helium underabundance. Thus we repeated the calculations described in step a) with the only two ODF tables evaluated for null helium abundance available and for metallicity equal to  $[M/H] = 0.0$  and  $-0.5$  dex (panels *b* and *c* of Figs. 1 and 2). The derived abundances and determined  $\xi$  are then used to compute a new ATLAS9 model. For model calculations, we used a step of 50 K for  $T_{\text{eff}}$  and 0.01 dex for  $\log g$ . A posteriori we found that smaller increments did not significantly change the  $\chi^2$  value.

The best fit was obtained for the model computed with the ODF for  $[M/H] = -0.5$ , zero helium abundance and:

$$T_{\text{eff}} = 12\,950 \pm 50 \text{ K}$$

$$\log g = 4.05 \pm 0.01$$

$$\xi = 0 \text{ km s}^{-1} \text{ with an error of } 0.7 \text{ km s}^{-1}.$$

The different results from using the two Balmer lines underlines the importance of using them simultaneously. In Table 1 we list, for each ODF used, the values obtained for  $T_{\text{eff}}$ ,  $\log g$  and  $\chi^2$  for the  $H_\delta$  and  $H_\gamma$  lines. The best match was obtained for the model computed with the ODF tabulated for  $[M/H] = -0.5$ , a null helium abundance and  $\xi = 0 \text{ km s}^{-1}$ . Moreover, we would like to focus the reader's attention on the  $\chi^2$  computed for each configuration. An important result is that for  $H_\delta$  the value of  $\chi^2$  changes considerably according to the adopted ODF, while in the case of  $H_\gamma$  changes are slight. Thus, we conclude that  $H_\delta$  is a better and more sensitive indicator of effective temperature and surface gravity than  $H_\gamma$ .

## 5. Abundance analysis

To derive the abundances we identified all the unblended lines, with the exception of helium, in the observed spectrum of HR 6000 using SYNTHE. The atomic parameters adopted in our analysis are from Kurucz' line lists<sup>2</sup>. From the measured equivalent widths, using the LTE code WIDTH9 (Kurucz 1993), we obtained the abundance values for each different ion by simply averaging the values obtained from each line. When, for a given element, a few unblended lines or multiplets were found we used SYNTHE to model them in order to obtain the abundance. Abundances are expressed in the usual form  $\log N_{\text{el}}/N_{\text{Tot}}$ .

To derive the rotational velocity, we used SYNTHE to reproduce the profiles of lines observed in the spectral window  $\lambda\lambda 4615\text{--}4640 \text{ \AA}$ . Contrary to the value of  $8 \text{ km s}^{-1}$  reported by Royer et al. (2002), our best match with the observations was achieved convolving the computed profiles with a stellar rotational profile having  $v_e \sin i = 0 \text{ km s}^{-1}$ . This result could be indicative of a very small angle between the line of sight and the rotational axis. In the hypothesis of the *Oblique*

**Table 1.** Estimated effective temperatures and gravities for HR 6000 for various metal opacity tables. For each line we list the  $\chi^2$  value. ATLAS9 models were computed for null microturbulence.

ODF		$H_\delta$			$H_\gamma$		
$[M/H]$	He	$T_{\text{eff}}$	$\log g$	$\chi^2$	$T_{\text{eff}}$	$\log g$	$\chi^2$
[0.0]	☉	13 150	4.02	1.19	12 750	3.95	0.56
[0.0]	0	13 250	4.13	1.13	13 000	4.11	0.50
[-0.5]	0	12 950	4.05	0.84	12 900	4.05	0.55

*Rotator Model* an almost null rotational velocity is consistent with the very long rotational period ( $P > 14$  years) estimated by van den Ancker et al. (1996) on the basis of photometric observations.

The radial velocity measurement was carried out using the aforementioned FeII lines, which gave a value of heliocentric  $RV = 0.67 \pm 0.38 \text{ km s}^{-1}$  on HJD = 2 452 516.498.

Below we describe and comment on the abundance analysis for each element in turn:

*Helium* – Neutral helium lines in a normal star with  $T_{\text{eff}} \approx 13\,000$  are usually strong, even if the maximum strength is reached for the spectral type B2. In the helium-poor star HR 6000, HeI lines are consequently weak and, in some cases, strongly affected by blends with metal lines, iron in particular. For instance, the important lines HeI  $\lambda\lambda 4388, 4471$  and  $4921 \text{ \AA}$  are so blended that they are not useful for abundance calculations. Hence, to investigate the helium abundance we attempted to reproduce, by spectral synthesis, the profiles of the only two lines easily observed, namely HeI  $\lambda\lambda 4713$  and  $5875 \text{ \AA}$ .

Leone & Lanzafame (1997) observed, among others, HeI  $\lambda 5875 \text{ \AA}$  in a sample of B-type stars with  $12\,000 \text{ K} < T_{\text{eff}} < 24\,000 \text{ K}$  and  $3.4 < \log g < 4.4$  and found that the equivalent widths of this line are adequately reproduced by the Auer & Mihalas (1973) and Dufton & Mckeith (1980) NLTE calculations. In general, LTE calculations underestimate equivalent widths.

Thus, because of the importance of NLTE effects, the synthetic helium lines were computed with the version 43 of the program SYNSPEC (Hubeny et al. 2000). This program reads the same input model atmosphere previously computed using ATLAS9 and solves the radiative transfer equation, wavelength by wavelength in a specified spectral range. SYNSPEC also reads the same Kurucz list of lines we used for the metal abundances. SYNSPEC allows one to compute the line profiles considering an approximate NLTE treatment even for LTE models. This is done by means of the second-order escape probability theory (for details see the paper by Hubeny et al. 1986). Moreover, the helium atom is considered explicitly and 14 levels of HeI are taken into account. For HeI  $\lambda\lambda 4713$  and  $5875 \text{ \AA}$ , detailed line broadening tables are taken from Dimitrijevic & Sahal-Brechot (1984).

The resulting abundance is  $\log N_{\text{He}}/N_{\text{Tot}} = -2.50$ .

*Carbon, nitrogen and oxygen* – Three lines of CII are useful in the visible range to infer carbon abundance (see for example Catanzaro & Leone 2002), namely: the multiplet at

<sup>2</sup> <http://kurucz.harvard.edu/LINESLIST/GFALL/gfall1.dat>

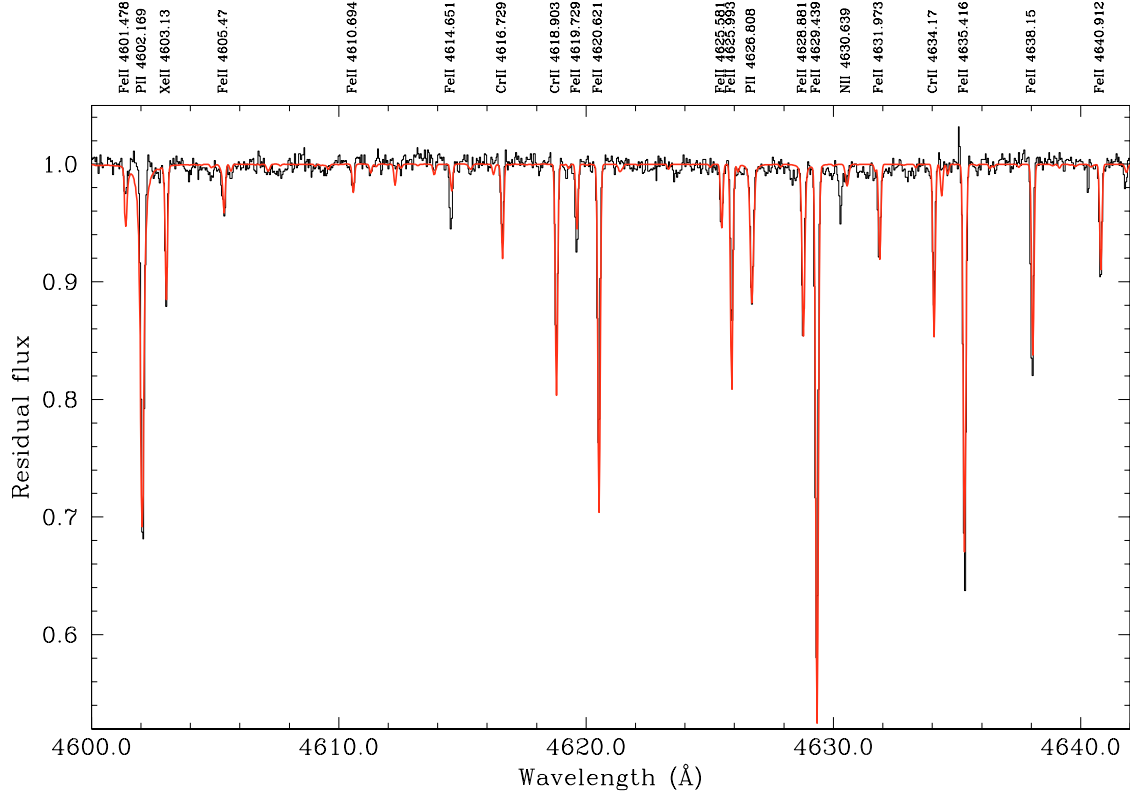


**Fig. 3.** As an example, a small portion of the observed spectrum is compared with the synthetic spectrum computed with the abundances derived in this study.

$\lambda 4267.261$  Å and the doublet at  $\lambda 6578.052$  and  $6582.882$  Å. The absence of these lines in our spectrum sets an upper limit for the carbon abundance to  $-5.60$ . This value is more than 2 dex underabundant with respect to the Sun. At the effective temperature adopted for HR 6000, a solar nitrogen abundance is not expected to generate strong spectral lines in the observed spectrum. Hence, we cannot derive its abundance and we assumed the Castelli et al. (1985) value. Finally, from the spectral synthesis of two On lines at  $\lambda 6155.971$  Å and  $\lambda 6157.755$  Å we derive an oxygen abundance of  $-3.80$ , about 0.7 dex lower than the Sun.

*Sodium* – The only NaI lines observed in our spectrum are the D lines at  $\lambda 5889.951$  Å and  $\lambda 5895.924$  Å. The problem concerning these lines is the strong contamination due to the ISM NaI lines. For this reason we could only set an upper limit for the sodium abundance equal to  $-4.64$ , that is about 1 dex larger than the solar case.

*Magnesium* – The magnesium abundance has been derived matching the MgII  $\lambda 4481$  Å line with a SYNTH profile. This line is actually a multiplet given by the fine structure transitions at  $\lambda 4481.126$ ,  $4481.150$  and  $4481.352$  Å. From these we found  $\log N_{\text{Mg}}/N_{\text{Tot}} = -6.00$ , which is  $\approx 1.5$  dex lower than the Sun.

*Aluminium* – The synthetic spectrum calculated for solar aluminium abundance predicts, among others, the presence of three lines of AlII at  $\lambda 6226.195$ ,  $6231.750$  and  $6243.367$  Å. Since these lines were not observed in our spectrum, we could fix  $-6.75$  as an upper limit for the aluminium abundance. This value corresponds to at least 1 dex lower than the solar case.

*Silicon* – This element is the most underabundant observed in HR 6000. As in the case of aluminium, a solar Si abundance should generate a number of spectral lines throughout the visible range. We selected seven of these lines in spectral regions where the signal-to-noise ratio is higher than 150, and we derive an upper limit of  $-7.15$  for the silicon abundance. That is more than 2.5 dex under the solar value.

*Phosphorus* – It is the most overabundant element in the atmosphere of HR 6000. Six spectral lines gave us  $\log N_{\text{P}}/N_{\text{Tot}} = -4.64 \pm 0.23$ , that is an overabundance of 2 dex with respect to the Sun.

*Sulfur* – This is another element for which only an upper limit could be fixed. Using the lines of SII at  $\lambda 4142.259$ ,  $4145.060$  and  $5014.042$  Å, we obtained  $\log N_{\text{S}}/N_{\text{Tot}} \leq -5.85$ , which is at least 1 dex lower than the Sun.

*Scandium* – An upper limit for the scandium abundance was found from the spectral synthesis of the ScII lines  $\lambda 4246.822$  and  $4320.732$  Å. We found  $-9.15$  that represents a moderate underabundance with respect to the Sun.

*Titanium* – We selected eleven unblended TiII lines, from which we derived a slight overabundance,  $\log N_{\text{Ti}}/N_{\text{Tot}} = -6.56 \pm 0.10$ , with respect to the Sun.

*Chromium* – Chromium is slightly overabundant with respect to the solar case. From ten unblended lines of CrII we obtain  $\log N_{\text{Cr}}/N_{\text{Tot}} = -6.25 \pm 0.08$ .

*Manganese* – We were able to infer the manganese abundance only from one spectral line, MnII  $\lambda 4326.639$  Å. From this line we obtained the value  $-5.60$ , about 1 dex larger than the Sun.

**Table 2.** Summary of the inferred abundances in the atmosphere of HR 6000. For comparison we reported the relative abundance in the solar photosphere Grevesse & Sauval (1998). According to these authors, xenon and mercury abundances are relative to the meteorites.

El	$\log N_{\text{el}}/N_{\text{Tot}}$	
	HR 6000	Sun
He	$-2.50 \pm 0.10$	-1.03
C	$\leq -5.60 \pm 0.10$	-3.51
O	$-3.80 \pm 0.10$	-3.20
Na	$\leq -4.64 \pm 0.15$	-5.70
Mg	$-6.00 \pm 0.10$	-4.45
Al	$\leq -6.75 \pm 0.11$	-5.56
Si	$\leq -7.15 \pm 0.37$	-4.48
P	$-4.64 \pm 0.23$	-6.58
S	$\leq -5.85 \pm 0.10$	-4.70
Sc	$\leq -9.15 \pm 0.10$	-8.83
Ti	$-6.56 \pm 0.10$	-7.01
Cr	$-6.25 \pm 0.08$	-6.36
Mn	$-5.60 \pm 0.10$	-6.64
Fe	$-3.98 \pm 0.20$	-4.53
Ni	$\leq -6.00 \pm 0.10$	-5.78
Xe	$-5.53 \pm 0.18$	-9.86
Hg	$\leq -8.00 \pm 0.10$	-10.90

*Iron* – Iron lines are the most numerous lines in the spectrum. We selected a number of unblended lines for three ionization stages: 2 lines of FeI, 96 lines of FeII and 5 lines of FeIII. From each ion we determined the corresponding abundance:  $-3.95 \pm 0.03$  from FeI,  $-3.98 \pm 0.20$  from FeII and  $-3.86 \pm 0.20$  from FeIII. Since these values all agree within the errors, we adopted their weighted average as the iron abundance in the atmosphere of HR 6000. Iron is about 1 dex more abundant than in the sun.

The fact that iron abundances obtained from lines of different ionization stages are in agreement led us to conclude that our adopted effective temperature is actually a good estimate and that iron is not vertically stratified along the atmosphere.

*Nickel* – Nickel lines are not expected to be very strong at the  $T_{\text{eff}}$  of our target. We selected three lines present in the  $\lambda$  5010–5020 Å spectral window; from these lines we obtained a slight underabundance of about 0.2 dex with respect to the Sun.

*Xenon* – Andersen et al. (1984) noted the presence of weak spectral lines in HR 6000 at the wavelengths of three XeII lines identified in  $\kappa$  Cnc by Aller (1970). They stated that the identification of their lines with XeII is supported at the 96% confidence level. In our analysis we confirm the existence of XeII lines, in particular we identify 5 of them, namely:  $\lambda$  4603.03 (Fig. 3), 4844.30, 5419.15, 5531.07 and 6051.15 Å. For these lines  $\log gf$  have been taken from the NIST database and data on level energies from Hirata & Horaguchi (1995). The Xe abundance we derived was  $-5.53 \pm 0.18$ . This value reflects an extreme xenon overabundance: more than 4 dex with respect to the abundances of the meteorites.

*Mercury* – Our spectrum allows us to fix an upper limit for the abundance of mercury. Through the synthesis of the spectral

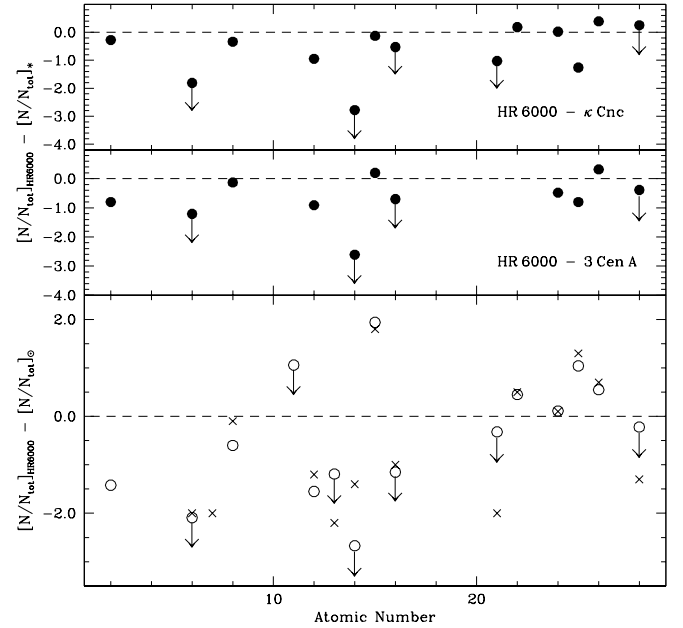


**Fig. 4.** In the bottom panel we compare the abundance pattern of HR 6000 here derived (Table 2) from visible data (open circles) with abundances derived from IUE data by Castelli et al. (1985) (crosses). With arrows we indicate the elements for which only an upper limit has been estimated. In the upper panels we report respectively the differences between our values and those reported by Adelman & Pintado (2000) for 3 Cen A, the prototype of He weak stars, and  $\kappa$  Cnc a typical HgMn star with effective temperature similar to that of HR 6000. For the sake of clarity, in this plot we did not report Xe and Hg abundances (see text).

region centered on HgII  $\lambda$ 3984 Å and 1 Å wide we obtained  $\log N_{\text{Hg}}/N_{\text{Tot}} \leq -8.00$ .

In Table 2 we summarize the inferred abundances for HR 6000 with their errors. For comparison we list also the corresponding solar standard values (Grevesse & Sauval 1998).

In Fig. 3 we show the comparison between observed and synthetic spectra in the spectral region  $\lambda$  4615–4642 Å. The synthetic spectrum has been computed using the abundances listed in Table 2.

Finally, in Fig. 4 we compare the abundance pattern of HR 6000 with the results of Castelli et al. (1985) obtained for the same object but using IUE data and with the abundances inferred for the He weak star prototype 3 Cen A and for  $\kappa$  Cnc a typical HgMn star with effective temperature close to that of HR 6000 (Adelman & Pintado 2000). For the sake of clarity, we have omitted Xe and Hg from the figure.

## 6. Discussion

Leone & Manfré (1997) have shown the importance of a correct abundance assumption in determining the  $T_{\text{eff}}$  and  $\log g$  values of a star by matching the observed  $H_{\beta}$  line. Extending their method, in the case of the He weak star HR 6000, we found that results are more accurately obtained by simultaneously matching the  $H_{\delta}$  and  $H_{\gamma}$  lines.

In Figs. 1 and 2 we show the importance of helium and metal abundances in determining  $T_{\text{eff}}$  and  $\log g$ . Neglecting

the correct He and metal abundances, two models, 400 K and 0.07 dex different in  $T_{\text{eff}}$  and gravity, are necessary (panels *a*). When we reduce helium leaving the metal content unchanged we decrease the mean molecular weight of the atmospheric material and thus the contributions to the electron pressure. Hence, we need to increase  $\log g$  in order to compensate for the helium deficiency (transition from panels *a* to panels *b*). The dependency on the effective temperature is less important than the gravity, with a difference in  $T_{\text{eff}}$  of about 2% from one model to another.

The abundance pattern inferred by us has been compared in Fig. 4 (bottom panel) with the value inferred from IUE data (Castelli et al. 1985). Inspecting Fig. 4 it is clear that even though the general pattern is essentially the same, there are some non-negligible differences. For instance, while for O, Al, Si, Sc and Ni we measured different abundances (discrepancies are up to 1.4 dex), for the other elements the inferred abundances agree quite well. There are two possible explanations for these discrepancies: *a*) different atmospheric model used for our calculations and *b*) vertical stratification of the elements. As to the model, Castelli and collaborators stated that the model they adopted,  $T_{\text{eff}} = 14\,000$  K and  $\log g = 4.00$  (Kurucz 1979), fulfils the ionization equilibrium criteria of several elements, iron in particular, although the UV continuum is slightly better reproduced by a model with  $T_{\text{eff}} = 13\,000$  K. The hypothesis of a vertical stratification could be supported from the consideration that UV and visible lines are formed in different layers. Furthermore the structure of the atmosphere assumed with their model is different from the one we computed with ATLAS9 code, hence given these differences, any conclusion about stratification should follow from an analysis performed with a consistent model in both ranges. This analysis will be the object of a future investigation.

In this paper, we show that with the correct assumption of abundances and opacity scale, we were able to compute a model that better reproduces Balmer lines and at the same time fulfils the ionization equilibria of FeI, FeII and FeIII.

In the upper panels of Fig. 4 we reported the differences between the abundances here inferred for HR 6000 and those reported by Adelman & Pintado (2000) for 3 Cen A (He weak prototype) and  $\kappa$  Cnc (HgMn). There is a general underabundance of elements in HR 6000 with respect to those two stars. In particular, the differences of carbon and silicon are lower by about one and two dex respectively. In Fig. 4 we did not include the abundances for Xe and Hg. Pintado et al. (1998) reported that the xenon abundance in three HgMn stars, with  $T_{\text{eff}}$  ranging from 13 125 K to 14 375 K, is between  $-5.22$  and  $-5.60$  dex. In particular, for  $\kappa$  Cnc, which has the lowest helium content and the  $T_{\text{eff}}$  closest to our target, the xenon abundance is compatible with the value we found for HR 6000.

## 7. Conclusion

The main purpose of this study was to investigate the sensitivity of important Balmer lines, such as  $H_{\delta}$  and  $H_{\gamma}$ , as good indicators of temperature and gravity in non-solar composition atmospheres. The technique was applied to the particular case of the chemically peculiar star HR 6000.

An ATLAS9 atmosphere model has been computed, adopting an ODF consistent as much as possible with the derived metal and helium abundances and the microturbulent velocity. Synthetic lines have been computed using SYNTH3, with the exception of HeI lines for which we used SYNSPEC.

Matching simultaneously  $H_{\delta}$  and  $H_{\gamma}$  we found the absolute minimum  $\chi^2$  when we used an ODF evaluated for null helium content and for  $[M/H] = -0.5$ . Moreover, we demonstrated that if a correct ODF is used in the model calculation, we obtained almost the same values for  $T_{\text{eff}}$  and  $\log g$  from the two lines. The adopted values of  $T_{\text{eff}}$  and  $\log g$  were 12 950 K and 4.05 dex, respectively. Finally, we noted also that  $H_{\delta}$  alone is a better indicator than  $H_{\gamma}$ , because the former is more sensitive to the ODF used.

With the aim of classifying this object, we also compared our abundances with the ones of two other stars: the prototype of He weak stars 3 Cen A and the HgMn star  $\kappa$  Cnc (Adelman & Pintado 2000).

The upper two panels of Fig. 4 show that the abundance pattern of HR 6000 is not similar to either of those classes of peculiarity. In particular, the silicon underabundance is difficult to explain even if we take into account the vertical stratification as a possible cause. Vauclair et al. (1979) and, later, Alecian & Vauclair (1981), for instance, have demonstrated that diffusion would produce a Si overabundance, as the Si stretches to float in the upper layers. We can conclude nothing about mercury as we could only fix an upper limit for its abundance, while we definitively confirm the presence of Xen lines in the spectrum.

Concerning iron, we did not find any evidence of vertical stratification, as the abundance derived from three ionization stages are, within the experimental errors, in agreement with each other.

In conclusion, HR 6000 seems to combine a number of abundance anomalies that usually appear separately in various classes of CP stars. It is very challenging to explain the presence of those anomalies all together in the same star, especially if we consider its likely very young age. The next step toward the understanding of the real nature of this object will be the combined analysis of the UV and optical spectrum, in order to verify the possible vertical stratification of the elements in the atmosphere.

## References

- Adelman, S. J., & Pintado, O. I. 2000, *A&A*, 354, 899
- Alecian, G., & Vauclair, S. 1981, *A&A*, 101, 16
- Aller, M. F. 1970, *A&A*, 6, 67
- Andersen, J., Jascheck, M., & Cowley, C. R. 1984, *A&A*, 132, 354
- Auer, L. H., & Mihalas, D. 1973, *ApJS*, 25, 433
- Bessel, M. S., & Eggen, O. K. 1972, *ApJ*, 177, 209
- Castelli, F., Cornachin, M., Hack, M., & Morossi, C. 1985, *A&AS*, 59, 1
- Catanzaro, G., & Leone, F. 2002, *NewA*, 7, 495
- Dimitrijevic, M. S., & Sahal-Brechot, S. 1984, *JQRST*, 31, 301
- Dufton, P. L., & McKeith, C. D. 1980, *A&A*, 81, 8
- Erspamer, D., & North, P. 2003, *A&A*, 398, 1121
- Farthmann, M., Dreizler, S., Heber, U., & Hunger, K. 1994, *A&A*, 291, 919
- Grevesse, N., & Sauval, A. J. 1998, *Space Sc. Rev.*, 85, 161

- Hirata, R., & Horaguchi, T. 1995, in *VizieR On-line Data Catalog: VI/69*. Originally published in: Department of Astronomy, Faculty of Science, Kyoto University, and, National Science Museum, 3-23-1 Hyakunin-cho, Shinjuku-ku, Tokyo
- Hubeny, I., & Lanz, T. 2000, *SYNSPEC - A user's guide*
- Hubeny, I., Harmanec, P., & Stefl, S. 1986, *Bull. Astron. Inst., Czechoslovakia*, 37, 370
- Kurucz, R. L. 1993, A new opacity-sampling model atmosphere program for arbitrary abundances, in *Peculiar versus normal phenomena in A-type and related stars*, IAU Coll. 138, ed. M. M. Dworetsky, F. Castelli, & R. Faraggiana, ASP Conf. Ser., 44, 87
- Kurucz, R. L., & Avrett, E. H. 1981, *SAO Special Report*, 391
- Kurucz, R. L. 1979, *ApJS*, 40, 1
- Leckrone, D. S., Fowler, J. W., & Adelman, S. J. 1974, *A&A*, 32, 237
- Leone, F., & Manfré, M. 1997, *A&A*, 320, 257
- Leone, F., & Lanzafame, A. C. 1997, *A&A*, 320, 893
- Norris, J. 1971, *ApJS*, 23, 213
- Pintado, O. I., Adelman, S. J., & Gulliver, A. F. 1998, *A&AS*, 129, 563
- Preston, G. W. 1974, *ARA&A*, 12, 257
- Royer, F., Gerbaldi, M., Faraggiana, R., & Gómez, A. E. 2002, *A&A*, 381, 105
- Thè, P. S., Tjin A Djie, H. R. E., Brown, A., et al. 1985, *Irish Astron. J.*, 17, 79
- Thè, P. S., & Tjin A Djie, H. R. E. 1978, *A&A*, 62, 439
- Tjin A Djie, H. R. E., & Thè, P. S. 1978, *A&A*, 70, 311
- van den Ancker, M. E., de Winter, D., & Thè, P. S. 1996, *A&A*, 313, 517
- Vauclair, S., Hardrop, J., & Peterson, D. A. 1979, *ApJ*, 277, 526
- Vidal, C. R., Cooper, J., & Smith, E. W. 1973, *ApJS*, 25, 37
- Zinnecker, H., & Preibisch, T. 1994, *A&A*, 292, 152